Available online at www.sciencedirect.com

ScienceDirect

MATTER AND RADIATION AT EXTREMES

Matter and Radiation at Extremes 1 (2016) 187–191

www.journals.elsevier.com/matter-and-radiation-at-extremes

Letter

Proton radiography of magnetic fields generated with an open-ended coil driven by high power laser pulses

Guoqian Liao [a,b], Yutong Li [a,b,e,*], Baojun Zhu [a,b], Yanfei Li [a,b], Fang Li [a], Mengchao Li [a,b], Xuan Wang [a], Zhe Zhang [a], Shukai He [c], Weiwu Wang [c], Feng Lu [c], Faqiang Zhang [c], Lei Yang [c], Kainan Zhou [c], Na Xie [c], Wei Hong [c], Yuqiu Gu [c,e], Zongqing Zhao [c], Baohan Zhang [c], Jie Zhang [d,e]

[a] *National Laboratory for Condensed Matter Physics, Institute of Physics, Chinese Academy of Sciences, Beijing 100190, China*

[b] *School of Physical Sciences, University of Chinese Academy of Sciences, Beijing 100190, China*

[c] *Science and Technology on Plasma Physics Laboratory, Laser Fusion Research Center, China Academy of Engineering Physics (CAEP), Mianyang 621900, China*

[d] *Key Laboratory for Laser Plasmas (MoE) and Department of Physics and Astronomy, Shanghai Jiao Tong University, Shanghai 200240, China*

[e] *Collaborative Innovation Center of IFSA (CICIFSA), Shanghai Jiao Tong University, Shanghai 200240, China*

Received 31 March 2016; revised 3 June 2016; accepted 8 June 2016

Available online 1 July 2016

Abstract

Recently generation of strong magnetic (B) fields has been demonstrated in capacitor coils heated by high power laser pulses [S. Fujioka et al., Sci. Rep. **3**, 1170 (2013)]. This paper will present a direct measurement of B field generated with an open-ended coil target driven by a nanosecond laser pulse using ultrafast proton radiography. The radiographs are analyzed with particle-tracing simulations. The B field at the coil center is inferred to be ~50 T at an irradiance of $\sim 5 \times 10^{14}$ W·cm^{-2}. The B field generation is attributed to the background cold electron flow pointing to the laser focal spot, where a target potential is induced due to the escape of energetic electrons.

PACS codes: 52.70.Ds; 52.50.Jm; 52.38.Fz

Keywords: Strong magnetic field; Laser-driven coil targets; Proton radiography

1. Introduction

Generation of strong magnetic (B) fields in free space has arisen increasing attention in material science [1], inertial confinement fusion [2], laboratory astrophysics [3] and other fields. The development of high-power lasers provides a new platform for producing strong B fields. Daido et al. demonstrated a B field of hundreds of teslas (T) with a capacitor coil target heated by high power laser pulses in the 1980s [4]. Recently Fujioka et al. have promoted the B field to the level of kT with laser energies of 1 kJ using similar targets [5].

In previous experiments, B-dot probes and the Faraday rotation method are used to measure the coil-induced B fields in free space [4–7]. B-dot probes can provide the evolution of B fields with a temporal resolution of tens-of-picoseconds. However, the local spatial distribution of B fields cannot be resolved. Since self-generated B fields could be excited at the

* Corresponding author. National Laboratory for Condensed Matter Physics, Institute of Physics, Chinese Academy of Sciences, Beijing 100190, China.

E-mail address: ytli@iphy.ac.cn (Y. Li).

Peer review under responsibility of Science and Technology Information Center, China Academy of Engineering Physics.

http://dx.doi.org/10.1016/j.mre.2016.06.003

laser focal spot due to the Biermann battery effect or other mechanisms simultaneously, the signal detected by the B-dot may be a combination of self-generated B field in the plasma and coil-induced B field in free space. In addition, the B-dot probe is vulnerable to the interference of the electromagnetic noise generated during relativistic laser–plasma interactions [8]. For the Faraday rotation measurement [9], one can obtain the local spatial distribution of B fields. However, it works only for a plasma region where the electron density is below the critical density of the optical probe. When one probes B fields in free space, there are also some limitations for Faraday rotation such as the blacking out of signals [5] and the uncertainty of Verdet constant with the increase of B fields.

Proton radiography can directly detect the temporal evolution and local spatial distribution of B or electrostatic (E) fields [10,11]. Relativistic laser-driven or implosion proton beams have been used to probe the fields localized in plasmas. In this paper, ultrafast proton radiography of the B fields generated in a coil target irradiated by a ns laser pulse is presented. An open-ended single coil [12], rather than a closed-loop capacitor coil reported before [4–7], is used as the B field generator. Proton radiographs are analyzed based upon particle-tracing simulations. A B field of ~50 T at the coil center is demonstrated at an irradiance of 5×10^{14} W·cm^{-2}. The B field is attributed to the return current of background cold electrons, rather than fast electrons.

2. Experimental setup

The experiment was carried out using the Xingguang-III facility at the Science and Technology on Plasma Physics Laboratory in Laser Fusion Research Center, CAEP. Fig. 1 shows the schematic of the experimental setup. The target used as the B field generator was an open-ended Cu coil with an inner diameter of 1 mm. The diameter of the Cu wire was 200 μm. One end of the wire was fabricated to be a planar target, which was normally irradiated by a 530 nm laser beam with an energy of 180 J and a duration of 1.1 ns. The focused laser intensity was ~5×10^{14} W·cm^{-2}. A proton beam was generated by using a 1 ps laser pulse to heat a 5 μm thick Cu foil via the target normal sheath acceleration. The incidence angle and the intensity of the short pulse were 20° and ~10^{19} W·cm^{-2}, respectively. Our previous measurements with similar targets [12] showed that the B field increased to its peak in 2–4 ns. Hence the ps laser pulse was launched at 4 ns after the irradiation of the ns laser beam. A stack of radiochromic films (RCFs) was used as the proton detector. It was wrapped with a 25 μm thick Al foil to shield from the laser light and other noises. Since the protons deposited most of their energy at the Bragg peak, each RCF layer provided a two-dimensional image of quasi-chromatic protons. The coil target and the RCF stack were placed 3 mm and 30 mm away from the proton target, respectively. This gave a magnification factor of 10. A nickel mesh with 600 lines per inch was set 1 mm away from the proton target.

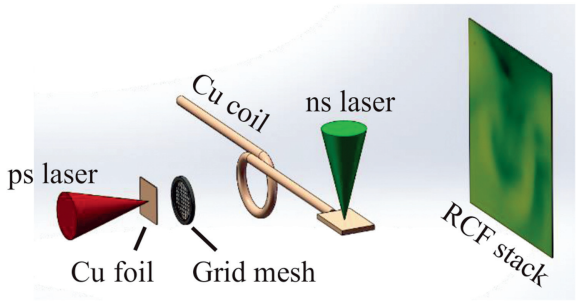

Fig. 1. Experimental setup of the face-on scheme. A ns laser beam was focused onto the planar target at the end of the coil to generate B fields. Another ps laser beam was focused onto a Cu foil to generate the proton beam. A stack of RCFs was used as the proton detector.

The B fields were measured in two geometrical schemes, the face-on (the proton beam perpendicular to the coil plane), and side-on (the proton beam parallel to the coil plane) geometries. We also tried using two B-dot probes to measure the B fields. However, it was difficult to extract the signal of B fields due to strong interferences of electromagnetic noises on the B-dots.

3. Results and discussions

3.1. Effect of the proton source size on the radiographs

The proton beam can be observed even on the 20th RCF layer, indicating that the maximum energy of the proton beam is >15 MeV. A typical face-on proton image is shown in Fig. 1. An unexpected feature is that the image of the mesh grid disappears in the whole field of view. Strong X-ray radiation will be generated when the planar target is heated by the ns laser pulse. The X-rays can ionize the rear surface of the Cu foil for proton generation, thus resulting in a heavily enlarged proton source size ρ [13] and the non-uniformity of proton beam profile. The source size has great effects on the contrast of the mesh grid. If the source size is too large, the mesh grid will be invisible on the RCFs.

The proton source size can be estimated by the knife-edge imaging technique [14]. Given that the diameter of the Cu wire (200 μm) is much larger than the source size, the Cu wire will behave like a knife-edge. The width of penumbral regions in the projection image of coils can be used to characterize the source size, which is inferred to be ~15 μm from the measured radiograph without the irradiation of the ns laser beam. The size is enlarged to be ~100 μm when the ns laser pulse is launched 4 ns earlier than the ps pulse. For such a large source size, the knife-edge approximation is inappropriate since it will underestimate the width of the penumbral region. This indicates that the lower limit of the real source size should be 100 μm.

The upper limit of the source size is estimated to be ~400 μm by the evolution of target rear sheath field, $\phi_{\mathrm{focus}} + c \cdot \tau_{\mathrm{L}}$, where ϕ_{focus} is the diameter of laser focal spot, c is the light velocity in vacuum and τ_{L} is the pulse duration of the ps laser beam. Therefore, the proton source size ranges from 100 μm to 400 μm. Both the enlarged proton source size

and some non-uniformity of the proton beam profile would lead to a blurry radiograph. A feasible way to mitigate the effect of the ns laser generated X-rays on the proton source is to add a several-microns-thick metal foil as an X-ray shield between the proton target and coil target, which will improve the quality of the proton source.

3.2. Identifying the current source for the B fields

The measured proton images for different proton energies (on different RCF layers) are similar. Fig. 2(a) shows a typical measured proton image for 8.0 MeV protons in the side-on geometry. The white dashed line illustrates the high proton density region. Compared with the proton images measured without the ns laser irradiation, the observed proton deflection near the Cu wire indicates that a B field is generated.

We used particle-tracing simulations to check the effect of the proton source size and retrieve the B fields from the proton radiographs. In the simulations, a loop coil is used to approximately model the experimental open-ended single-turn coil. The proton source, grid mesh, coil current and detector are set with a similar geometrical configuration to the experiment. Three parameters are variable in the simulations, the proton energy E_p, the proton beam source size ρ, and the coil current I.

Fig. 2(c)–(d) show the proton profiles obtained in simulations, which illustrate the proton deflection by B fields for two coil currents flowing in reversed directions. The protons propagate perpendicularly into the paper plane. The directions of I and B fields are also illustrated in the figures. The current I is set to be 50 kA. When passing through the B fields, no matter in which direction the coil current is, protons on one side will be repelled, while on the other side will be attracted. This results in a pear-like bubble structure, which is quasi-symmetrical in the vertical (upper-lower) direction, while asymmetrical in the horizontal (left-right) direction. The orientation of bubbles is dependent on the direction of the current I. Comparing the experimental image with simulations, one can infer that the B field generated inside the coil is in the upward direction. This indicates that a current flows away from the laser focus along the Cu wire, as sketched in Fig. 2(b). Therefore, the background cold electron return current driven by the positive potential of the target, rather than the energetic fast electrons themselves, is responsible for the generation of the B field.

Proton stopping by the wire, proton beam non-uniformity, or E fields located in the plasma sheath around the wire due to the ionization of strong X-ray or resistive heating may also have influences on the proton images. Proton stopping and beam non-uniformity should be closely related to the proton

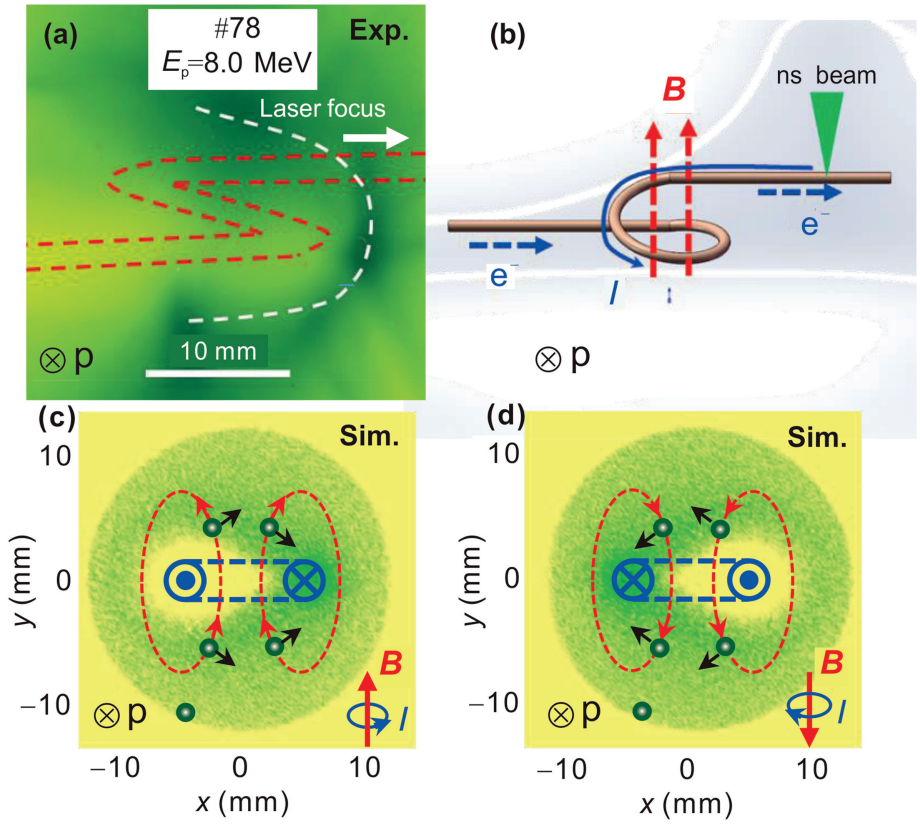

Fig. 2. (a) Experimentally measured side-on RCF image. The red dashed lines and white dashed line represent the contour of the coil and the high proton density region, respectively. (b) Schematic showing the electrons, current, and induced B fields. (c–d) Simulated proton density profiles with coil-current B fields, and schematics illustrating the proton deflection by B fields. The B field inside the coil is in (c) $+y$ and (d) $-y$ direction. The blue dashed lines, red dashed lines and black arrows in (c) and (d) sketch the projection of the coil, B fields and the proton deflection, respectively. The protons propagate inward for all figures.

energies. While the measured proton patterns show similar structures on different RCF layers. Since the E fields are distributed radially along the wire, the protons would be expelled away from the wire perpendicularly by the E fields, resulting in a "fat" coil shadow. This does not agree with the asymmetrical pear-like pattern in the horizontal direction.

The difference of the proton profiles in Fig. 2(a) and (c) could be due to different detailed magnetic topologies in the experiment and simulations especially at the coil opening end. The uncertainty of ρ in simulations will also lead to a large uncertainty of simulated proton images. Besides, the profile structure in Fig. 2(a) is not regular. Given those factors above, it is difficult to compare Fig. 2(a) with Fig. 2(c) quantitatively. We will use the face-on geometry to infer the amplitude of B fields.

3.3. Diagnosing the amplitude of B fields

Fig. 3(a) shows an experimentally measured RCF image of 8.0 MeV protons in the face-on geometry. The blue solid curve of Fig. 3(b) shows the lineout of the radial proton density along the white arrow in Fig. 3(a). The valley-peak distance in the radial distribution, defined as L, is used to characterize the proton deflection by the B fields. Due to the inherent asymmetry of the coil target, it is infeasible to average the radial proton density over the coil ring. Given the complicated B fields topology at the upper opening end and similar B fields in the horizontal plane to the simulations, we have mainly investigated the proton distribution in the horizontal direction. We find that Ls read from the left side and the right side of the proton images are almost the same. The measured L is ~(3.1 ± 0.2) mm for 8.0 MeV protons.

We have simulated the proton density distributions with different I and ρ. In the face-on case, when propagating near the coil wires, the protons will feel a Lorenz force pointing away from the coil. Such a B-fields-induced repulsion effect makes the size of the wire shadow look larger than the original wire diameter, as shown in Fig. 3(a). The dashed/dash dotted curves in Fig. 3(b) show the simulated proton distribution in radial direction with $I = 50$ kA. The value of simulated L with ρ in a range of 100–400 μm is ~(3.2 ± 0.4) mm, similar to the experiment result. Therefore, one can infer the coil current I to be ~50 kA, and the magnetic field B_0 at the center of the coil to be ~52 T. According to the spatial distribution of the calculated B field, the magnetic energy in the coil volume of 10 mm × 10 mm × 10 mm is calculated to be 1.9 J. Considering the ns pump laser energy to be 180 J, the corresponding energy conversion efficiency from laser to magnetic fields is ~1.0%.

Since the time of flight of the protons with specific energies to the coil is different, one can obtain time-resolved images in a single shot principally. In our experiment the time interval between 4 MeV and 15 MeV protons is about 40 ps. The characteristic time for the ns laser-driven B fields is at least on the order of ns [5,7,12]. Hence the B field sampled by the protons with different energies is nearly constant in our experiment.

For previous capacitor-coil targets, Santos et al. found that energetic electrons escaping from the rear disk irradiated by the laser pulses can reach to the facing coil and be magnetically trapped [7]. The induced electrostatic field by trapped electrons may affect the deflection of protons. While for our open-ended coil targets, the thick planar target irradiated by the ns laser pulse lines up with the coil. Due to the blocking and geometrical layout of the thick planar target, few of the escaped electrons or plasma plume can reach the coil. Therefore, the electrostatic effect of energetic electrons escaping from the ablation region is negligible in our case.

It should be pointed out that the amplitude of B fields might be overestimated from the face-on geometry, since either the proton deflection by E fields at the wire sheath or wire expansion caused by resistive heating hasn't been taken into account. Nevertheless, the side-on measurements have demonstrated that the B field is indeed generated by the laser-irradiated coil.

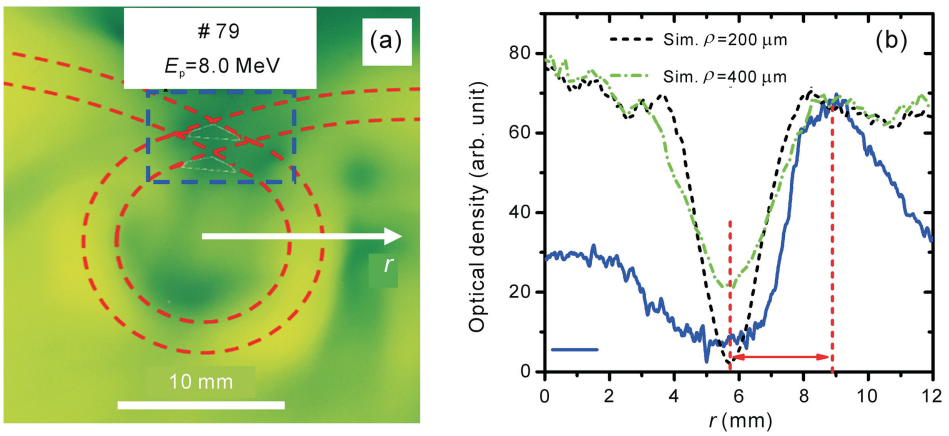

Fig. 3. (a) Measured RCF image of 8.0 MeV protons in the face-on geometry. The red dashed lines represent the coil contour. (b) Experimental (blue solid) and simulated (dashed/dashed dotted) proton density radial distributions. $I = 50$ kA, $\rho = 200$ μm (black dashed) and $I = 50$ kA, $\rho = 400$ μm (green dashed dotted) are used in the simulations.

4. Conclusions

Proton radiography is used to diagnose B fields generated from ns laser-irradiated open-ended, single-turn coil targets. The B fields are quantitatively retrieved with particle-tracing simulations. The B field at the center of the coil is ~50 T. The identified current source in a direction away from the laser focal spot indicates that the background cold electrons induced by the target potential play an important role in the B field generation. Further investigations on the dynamics and scaling of return currents in coils will be the subject of our future experiments. The B fields could be enhanced further by increasing the pump laser energy and optimizing the coil target design. The open-ended coil targets are simple and easy to be fabricated. The laser-induced B fields could provide a potential user-friendly experimental platform for studying magnetic-associated physics, especially laboratory astrophysics.

Acknowledgements

We would like to thank the Xingguang-III facility team at CAEP for laser operation and technical support, and thank H. Li from CAEP for helpful discussions on particle-tracing simulations. This work is supported by the National Basic Research Program of China (Grant No. 2013CBA01501), the National Nature Science Foundation of China (Grant Nos. 11135012, 11520101003 and 11375262), and the National High Technology Research and Development Program of China.

References

[1] D. Lai, Matter in strong magnetic fields, Rev. Mod. Phys. 73 (2001) 629.
[2] W.-M. Wang, P. Gibbon, Z.-M. Sheng, Y.-T. Li, Magnetically assisted fast ignition, Phys. Rev. Lett. 114 (2015) 015001.
[3] B. Albertazzi, A. Ciardi, M. Nakatsutsumi, T. Vinci, J. Béard, et al., Laboratory formation of a scaled protostellar jet by coaligned poloidal magnetic field, Science 346 (2014) 325.
[4] H. Daido, F. Miki, K. Mima, M. Fujita, K. Sawai, et al., Generation of a strong magnetic field by an intense CO_2 laser pulse, Phys. Rev. Lett. 56 (1986) 846.
[5] S. Fujioka, Z. Zhang, K. Ishihara, K. Shigemori, Y. Hironaka, et al., Kilotesla magnetic field due to a capacitor-coil target driven by high power laser, Sci. Rep. 3 (2013) 1170.
[6] C. Courtois, A.D. Ash, D.M. Chambers, R.A.D. Grundy, N.C. Woolsey, Creation of a uniform high magnetic-field strength environment for laser-driven experiments, J. Appl. Phys. 98 (2005) 054913.
[7] J.J. Santos, M. Bailly-Grandvaux, L. Giurida, P. Forestier-Colleoni, S. Fujioka, et al., Laser-driven platform for generation and characterization of strong quasi-static magnetic fields, New J. Phys. 17 (2015) 083051.
[8] A. Poyé, S. Hulin, M. Bailly-Grandvaux, J.-L. Dubois, J. Ribolzi, et al., Physics of giant electromagnetic pulse generation in short-pulse laser experiments, Phys. Rev. E 91 (2015) 043106.
[9] J.A. Stamper, B.H. Ripin, Faraday-rotation measurements of megagauss magnetic fields in laser-produced plasmas, Phys. Rev. Lett. 34 (1975) 138.
[10] M. Borghesi, A. Schiavi, D.H. Campbell, M.G. Haines, O. Willi, et al., Proton imaging detection of transient electromagnetic fields in laser-plasma interactions, Rev. Sci. Instrum. 74 (2003) 1688.
[11] C.K. Li, F.H. Séguin, J.A. Frenje, J.R. Rygg, R.D. Petrasso, et al., Monoenergetic proton backlighter for measuring E and B fields and for radiographing implosions and high-energy density plasmas, Rev. Sci. Instrum. 77 (2006), 10E725.
[12] B.-J. Zhu, Y.-T. Li, D.-W. Yuan, Y.-F. Li, F. Li, et al., Strong magnetic fields generated with a simple open-ended coil irradiated by high power laser pulses, Appl. Phys. Lett. 107 (2015) 261903.
[13] A.J. Mackinnon, M. Borghesi, S. Hatchett, M.H. Key, P.K. Patel, et al., O. Willi, Effect of plasma scale length on multi-MeV proton production by intense laser pulses, Phys. Rev. Lett. 86 (2001) 1769.
[14] M. Borghesi, A.J. Mackinnon, D.H. Campbell, D.G. Hicks, S. Kar, et al., Multi-MeV proton source investigations in ultraintense laser-foil interactions, Phys. Rev. Lett. 92 (2004) 055003.